# BPSK-based MIMO FMCW Automotive-Radar Concept for 3D Position Measurement

Yoke Leen Sit, Gang Li, Sarath Manchala, Hamid Afrasiabi, Christian Sturm, Urs Lübbert

Active Safety Systems Product Line

VALEO Schalter und Sensoren GmbH, Bietigheim-Bissingen, Germany

{leen.sit | gang.li2| sarath.manchala | hamid.afrasiabi | christian.sturm | urs.luebbert}@valeo.com

***Abstract* — A novel concept of employing BPSK codes to achieve a simultaneous transmission in a 79 GHz FMCW automotive radar is presented in this paper. With a MIMO topology, simultaneous azimuth and elevation measurements become possible by utilizing the angle-dependent phase difference between the antenna arrays. Hence, this approach can offer a 4D detection of range, azimuth, elevation and Doppler-velocity for each detected target. This concept has been verified through test drives in multiple scenarios and the measurements showed that the elevation accuracy is only limited by calibration.**

***Keywords* — 3D position, Automotive Radar, BPSK, Elevation, FMCW, MIMO**

## I. INTRODUCTION

As driver assistance systems become more and more sophisticated, it is expected that the radar sensors, which function as the 'eyes' of the vehicle, will also evolve in parallel. One of the evolutions demanded from radars is the ability to discriminate multiple targets especially for the discernment of vulnerable road users, namely the pedestrians. Automotive radars currently already possess the ability to provide a three-dimensional (3D) detection in range, cross-range (azimuth) and Doppler. For better range resolution and hence accuracy, an agile or large signal bandwidth is also employed [1, 2]. In recent years, radar-based automatic parking or autonomous driving becomes popular in automotive development, e.g, to distinguish vulnerable road user (pedestrian or bicyclist) for active safety or to classify the over-rideable object such as curbs for automatic parking. As such the elevation information is highly recommended and helpful in the sensor's signal processing.

While a beam steering technique can produce the desired four-dimensional (4D) discrimination of multiple targets via scanning, this technique is unsuitable for moving vehicles due to the timing efficiency, which may consequently result in blind spots.

The current popular approach uses multiple antennas, optimized in their arrangement, to produce an overall array with a radiation pattern that is also optimized in terms of accuracy and angular resolution. The conditions to this multiple-input multiple-output (MIMO) approach are: 1) the simultaneous transmission of signals from the multiple transmitters, and 2) the separability of the transmit waveforms at all receivers. With this approach, the signal-to-noise ratio (SNR) at each receive antenna will increase by 6dB with each additional transmit antenna used where, 3 dB arises from the transmit power plus another 3 dB of processing gain for each transmitter. This increase in SNR will no doubt will enhance the detection of the pedestrians further.

For such a concept to work, the chosen waveform must be uncorrelated. This can be achieved using frequency or code multiplexed waveforms. An example is the Orthogonal Frequency Division Multiplexing (OFDM)-based MIMO radar presented with a proof-of-concept in [3, 4]. While the OFDM waveform provides more degrees of freedom to cater to a larger number of transmit antennas, it is undeniably expensive to implement due to the requisite of a large instantaneous bandwidth. For automotive radars, with hardware cost efficiency and technological maturity being the priority, the Frequency Modulated Continuous Wave (FMCW) fast-chirp modulation is still predominant. Hence, a code-multiplexed solution is preferred. In this paper, a simple FMCW waveform coding based on the Bipolar Phase Shift Keying (BPSK), which requires only minimal effort in the waveform generation and decoding, is presented.

The BPSK coding on the FMCW wave presented here involves transmitting all chirps with 0° phase modulation on one transmitter and an alternate of 0° and 180° phase modulation on every alternate chirp for the second transmitter. This method, while simple in implementation, also gives rise to Doppler ambiguities due to the emergence of multiple peaks in the spectrum. Restricting this method to only two transmit antennas with an arbitrary number of receive antennas, we present in this paper a method to resolve the Doppler ambiguities in the next sections without any loss of information. Using two sets of antenna arrays positioned along the azimuth and elevation, the proof of concept for elevation detection feasibility is presented, thus paving the way for an enhanced 4D radar.

The paper is organized as follows. Section I presents the introduction, followed by the FMCW concept in Section II. Section III then presents the BPSK-coded waveform. In Section IV the key parameters, measurement setup and results of the proposed radar are detailed. Section V then concludes this paper.

## II. BURST-SEQUENCE FMCW SIGNALWAVEFORM

As shown in Fig. 1, the instantaneous frequency $f_c(t)$ of the linear down-sweep FMCW signal waveform

$$f_c(t) = f_{c0} - \frac{B}{T}t = f_{c0} - \mu t, \tag{1}$$

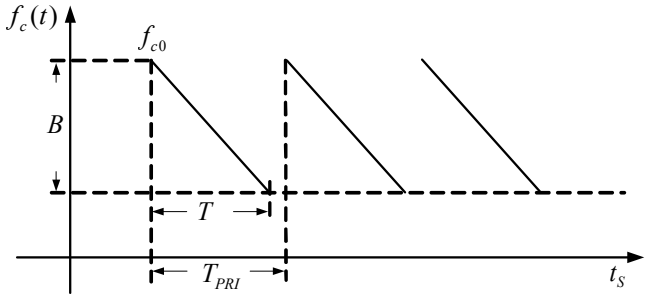


Fig. 1. Illustration of the burst-sequence FMCW signal waveform, where $f_{c0}$, $B$, $T$ and $T_{\mathrm{PRI}}$ indicate the carrier-frequency, bandwidth, sweep-duration and pulse repetition duration, respectively.

where $f_{c0}$, $\mu$, $T$, $T_{\mathrm{PRI}}$, $t$, and $t_s$ are the carrier-frequency, sweep-rate, sweep duration, pulse repetition interval, the time variable of one single sweep and the pulse repetition interval, respectively.

Mathematically, the transmitted signal $s_{\mathrm{Tx}}(t)$ with the instantaneous phase $\varphi_c(t)$, i.e., the integral over the sweep radial frequency $f_c(t)$, can be expressed as follows,

$$\begin{aligned} s_{\mathrm{Tx}}(t) &= A_{\mathrm{Tx}} \cdot \cos\left(\int_0^t 2\pi f_c(t)\, dt\right) \\ &= A_{\mathrm{Tx}} \cdot \cos(2\pi f_{c0} t - \pi\mu t^2 + \varphi_{c0}). \end{aligned} \tag{2}$$

$\varphi_{c0}$ is the initial value of the instantaneous phase. For simplification, the variable $A$ with various subscripts is used to represent the signal strength, e.g., $A_{\mathrm{Tx}}$, $A'_n$, and $A_n$ in (3-7). The back-scattered signal $s_{\mathrm{back}}(t)$ is environment dependent, hence $\tau_n$ is used to represent the RTOF (round-trip time of flight) of the $n^{\mathrm{th}}$ target, e.g., infrastructure or moving vehicles and is depicted as,

$$s_{\mathrm{back}}(t) = A'_n \cdot s_{\mathrm{Tx}}(t - \tau_n), \tag{3}$$

The mixed signal received by one receiver antenna is a simple multiplication of,

$$\begin{aligned} s_{\mathrm{Mix}}(t) &= s_{\mathrm{back}}(t) \cdot s_{\mathrm{Tx}}(t) \\ &= A'_n \cdot s_{\mathrm{Tx}}(t - \tau_n) \cdot s_{\mathrm{Tx}}(t). \end{aligned} \tag{4}$$

In the case of a short-range radar, the quadratic phase term in (4) can be ignored. With a well-designed low-pass filter, the mixed signal in time-domain can be simplified as,

$$s_{\mathrm{Mix}}(t) \cong A_n \cdot \cos(2\pi\mu\tau_n t - 2\pi f_{c0}\tau_n) \tag{5}$$

Now the mixed signal can be easily expressed with Euler's formula due to the IQ-mixer, using,

$$s_{\mathrm{Mix}}(t) \cong A_n \cdot e^{j2\pi\mu\tau_n t} \cdot e^{-j2\pi f_{c0}\tau_n}. \tag{6}$$

Hence, the beat-signal in frequency domain can be expressed as follows, where $w(t)$ represents a window function, e.g., a Hamming window.

$$\begin{aligned} S_{\mathrm{Mix}}(f_{\mathrm{range},n}) &= \mathcal{F}\{s_{\mathrm{Mix}}(t) \cdot w(t)\} \\ &= \mathcal{F}\{A_n \cdot e^{j2\pi\mu\tau_n t} \cdot e^{-j2\pi f_{c0}\tau_n}\} \\ &\quad * W(2\pi f_{\mathrm{range},n}) \\ &= A_n \cdot e^{-j2\pi f_{c0}\tau_n} \cdot \delta(2\pi\mu\tau_n) * W(2\pi f_{\mathrm{range},n}) \\ &= A_n \cdot W\left(2\pi\left(f_{\mathrm{range},n} - \mu\tau_n\right)\right) \cdot e^{-j2\pi f_{c0}\tau_n}. \end{aligned} \tag{7}$$

Here, $\mathcal{F}\{\cdot\}$, $*$, $\delta(\cdot)$, and $W(f)$ represent the Fourier-transform, convolution operator, Dirac-function and window function in frequency domain, respectively.

## III. BPSK-MIMO Concept for Elevation Estimation

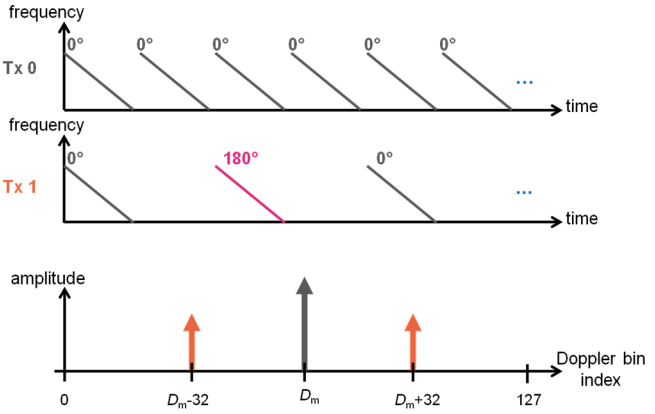


Fig. 2. (top) BPSK-MIMO waveform synthesizer of two transmit-antennas. (bottom) Doppler spectrum for a stationary target resulting from both waveforms assuming 128 sweeps.

Within a short time interval of one radar snapshot, where in this case consists of 128 sweeps, the total measurement duration is a few milliseconds. The RTOF of a target can be approximately considered as

$$\tau_n \approx \tau_0 + v_D \cdot K \cdot T_{\mathrm{PRI}}, \quad \text{where,} \tag{8}$$

$v_D$ is the Doppler velocity, $K$ is the number of sweeps and $\tau_0$ is the initial RTOF. The FFT in the slow time direction due to the waveform of Tx1 becomes,

$$\begin{aligned} &S_{\mathrm{Mix,Tx1}}(f_{range,n}, f_{\mathrm{D}}) \\ &= \mathcal{F}\left\{A_n \cdot W\left(2\pi\left(f_{\mathrm{range},n} - \mu\tau_n\right)\right) \cdot e^{-j2\pi f_{c0}\tau_n}\right\} \\ &\quad * W(2\pi f_{\mathrm{D}}) \\ &= A_n \cdot W\left(2\pi\left(f_{\mathrm{range},n} - \mu\tau_0\right)\right) \cdot e^{-j2\pi f_{c0}\tau_n} \\ &\quad \cdot \delta(2\pi f_{c0} K T_{\mathrm{PRI}} v_D) * W(2\pi f_{\mathrm{D}}) \\ &= A_n \cdot W\left(2\pi\left(f_{\mathrm{range},n} - \mu\tau_0\right)\right) \\ &\quad \cdot W(2\pi(f_{\mathrm{D}} - f_{c0} K T_{\mathrm{PRI}} v_D)) \cdot e^{-j2\pi f_{c0}\tau_n} \end{aligned} \tag{9}$$

In this paper, the MIMO concept is achieved using a code-multiplex (Fig. 2) approach to transmit multiple signals

simultaneously. Since the signal mixing is the same in the time and frequency domains, only the frequency modulation of the BPSK part is of interested. The modulation in Doppler direction causes the periodic repetition in the frequency domain. Using a factor $k_e$ of 4, the Doppler-frequency modulation is bi-directionally shifted by

$$f_{\mathrm{D,BPSK}} = f_{\mathrm{D}} \pm \frac{K}{k_e} f_{\mathrm{D}}. \tag{10}$$

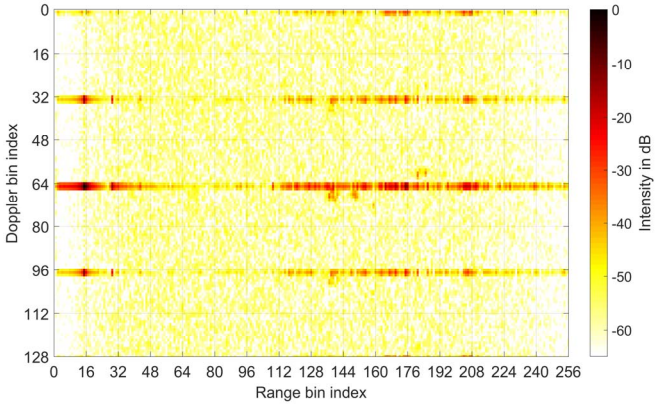


Fig.3. Proof of the MIMO concept through measurement with static target scenario: The image intensity shows the normalized range-Doppler spectrum, the x-axis and y-axis represent the range and Doppler indices, respectively.

Fig. 3 shows the measured results, where the Doppler bin 64 belongs to the detections of Tx0 (see Fig. 2), whereby, the target at Doppler bin 64 indicates zero velocity. The detection of the same static target due to Tx1 appears at Doppler bin 32 and 96, where the power of these BPSK-coded peaks is attenuated by 6dB compared to the main peak at Doppler bin 64. In this way the correct Doppler-velocity can be distinguished among the resulting three peaks.


Fig.4. Valeo test car with radar sensors were mounted at the corners angled at ±45°, respectively.

## IV. Measurement Results

As shown in Fig. 4, four midrange radar sensors were mounted at the corners of the vehicle with the mounting angle ±45° respectively. The height of the sensors is 50 cm above the ground. Each sensor has two transmit-antennas (oriented vertically for elevation detection) and a four-receiver antenna array (oriented horizontally for azimuth detections). Hence each sensor has 8 virtual antenna elements.

In this test, the FMCW signal bandwidth is set to 1.6 GHz and with the carrier frequency of 79 GHz. Therefore, the resolution in range direction is 0.09 m and maximum unambiguous Doppler-velocity is approximately 15 m/s. The vehicle was driven at around 10 km/h, therefore, the Doppler-ambiguity issue was not considered in this test. Generally, the Doppler-ambiguity due to high velocities can be solved by using Chinese reminder theorem [5].

Comparing to the measured static results in Fig. 3, the measurement with the sensors mounted on the test vehicle validates the feasibility of the BPSK-coded MIMO concept.

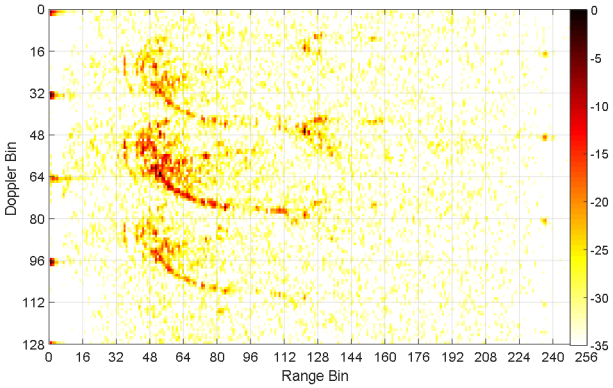


Fig.5. Normalized range-Doppler spectrum based on BPSK-MIMO concept measured with Valeo test vehicle.

The elevation estimation starts after the generation of the spectrum as depicted in Fig. 5 followed by a Constant False Alarm Rate (CFAR) algorithm detection [6,7] to distinguish probable targets from noise. The detected peaks in Fig. 5 can be distinguished by the difference in power of 6 dB as shown in Fig.2 (bottom). The peak with the highest power belongs to Tx0 while the other pair peaks with -6 dB power relatively belongs to Tx1. Details are given in [8]. The phase difference of the $n^{\mathrm{th}}$detected target between the two vertically-oriented transmit antennas $\psi_n$, is elevation angle $\theta_n$ dependent, and is given by the following relation,

$$\psi_n \quad \propto \quad \theta_n = \sin^{-1} \frac{R_n}{H_n}. \tag{11}$$

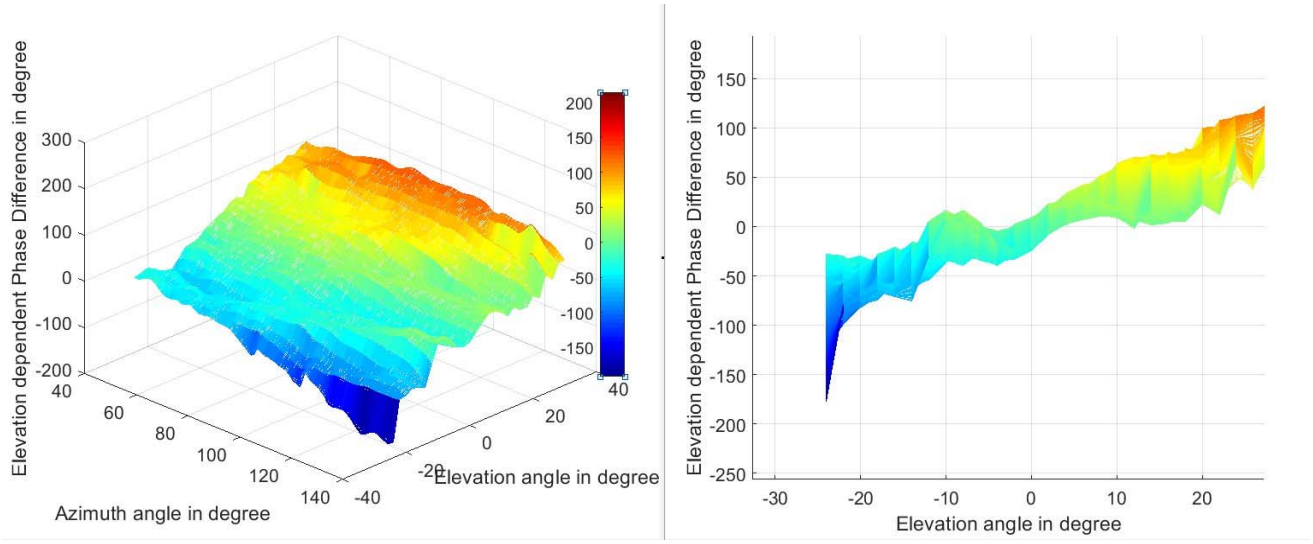


Fig.6. 3D Measurement results of elevation-dependent phase difference using a 10 dBsm corner reflector as the sole target.

with $R_n$ and $H_n$ being the detected range and height of the $n^{\text{th}}$ target respectively. As such, a phase difference vs. elevation angle curve chart is needed in order to translate the detected $\psi_n$ into height information. This chart can be obtained by performing 3D measurements using a single 10 dBsm corner reflector located at a predefined range over all possible azimuth and elevation angles. In this paper, the 3D measurement was performed with the sensor integrated on the car, behind a bumper. The results are shown in Fig. 6.

It can be seen that the phase difference rises linearly with the corresponding elevation angles. There are however uncertainties or deviation of the phase difference over a single elevation angle point as evident in Fig. 6 (right), as the phase difference deviates over the measured azimuth angles as well. These uncertainties arise mainly due to the signal diffraction from the bumper. It is very common then for the next step to be a calibration during the sensor integration into the vehicle to improve the accuracy of these curves.

## V. Conclusion

In order to achieve 4D detection comprising range, azimuth, elevation and Doppler for a conventional automotive radar using FMCW with fast chirps, additional antennas or arrays oriented vertically are required. Moreover, the transmit antennas must be able to transmit uncorrelated waveforms simultaneously so that the signals can be distinguished at the receivers. Hence a BPSK-coded waveform for the FMCW was proposed as a measure which does not require extensive hardware and signal processing effort.

The work in this paper has proven that while the BPSK coding leads to multiple peaks in the spectrum, they can easily be resolved. Using this information as well, the phase difference between the two transmitted signals can be used to estimate the elevation angle and subsequently the height of the detected target.

Using radar sensors mounted on a test vehicle and performing a test in various driving scenarios, it has been shown that a 4D detection is indeed possible with reasonably good results. The challenge for the next step is clearly the calibration of the phase difference vs. elevation angle curves, which sets the limits of the elevation angle estimation accuracy here.

## References


[1] Winkler, Volker. "Range Doppler detection for automotive FMCW radars." In *Microwave Conference, 2007. European*, pp. 1445-1448. IEEE, 2007.

[2] C. Sturm, G. Li, G. Heinrich, U. Lübbert, "79 GHz Wideband Fast Chirp Automotive Radar Sensor with Agile Bandwidth", *Proc. of the IEEE MTT-S International Conference on Microwaves for Intelligent Mobility (ICMIM)*, San Diego, CA, May 2016.

[3] Sit, Yoke Leen, Thuy T. Nguyen, and Thomas Zwick. "3D Radar imaging with a MIMO OFDM-based radar." *Microwave Conference Proceedings (APMC), 2013 Asia-Pacific*. IEEE, 2013.

[4] Sit, Yoke Leen, Benjamin Nuss, Sanjoy Basak, Mateusz Orzol, Werner Wiesbeck, and Thomas Zwick. "Real-time 2D+ velocity localization measurement of a simultaneous-transmit OFDM MIMO Radar using Software Defined Radios." In *Radar Conference (EuRAD), 2016 European*, pp. 21-24. IEEE, 2016.

[5] Wojtkiewicz, Andrzej, et al. "Two-dimensional signal processing in FMCW radars." *Proc. XX KKTOiUE* (1997): 475-480.

[6] Rohling, Hermann. "Radar CFAR thresholding in clutter and multiple target situations." *IEEE transactions on aerospace and electronic systems* 4 (1983): 608-621.

[7] Kronauge, Matthias, and Hermann Rohling. "Fast two-dimensional CFAR procedure." *IEEE Transactions on Aerospace and Electronic Systems* 49.3 (2013): 1817-1823.

[8] Christian Sturm, Yoke Leen Sit, Gang Li, Hamid Afrasiabi, Urs Lübbert "Automotive Fast-Chirp MIMO Radar with Simultaneous Transmission in a Doppler-Multiplex", *Proc. 19th International Radar Symposium, IRS 2018,* (to be published), June 2018.